Tuning chemical compositions of bimetallic AuPd catalysts for selective catalytic hydrogenation of halogenated quinolines

Sai Zhang,[a] Zhaoming Xia,[a] Ting Ni,[a] Huan Zhang,[a] Chao Wu[a] and Yongquan Qu[a]*

[a] Frontier Institute of Science and Technology and State Key Laboratory for Mechanical Behavior of Materials, Xi'an Jiaotong University, Xi'an, 710049, China

** E-mail: yongquan@mail.xjtu.edu.cn*

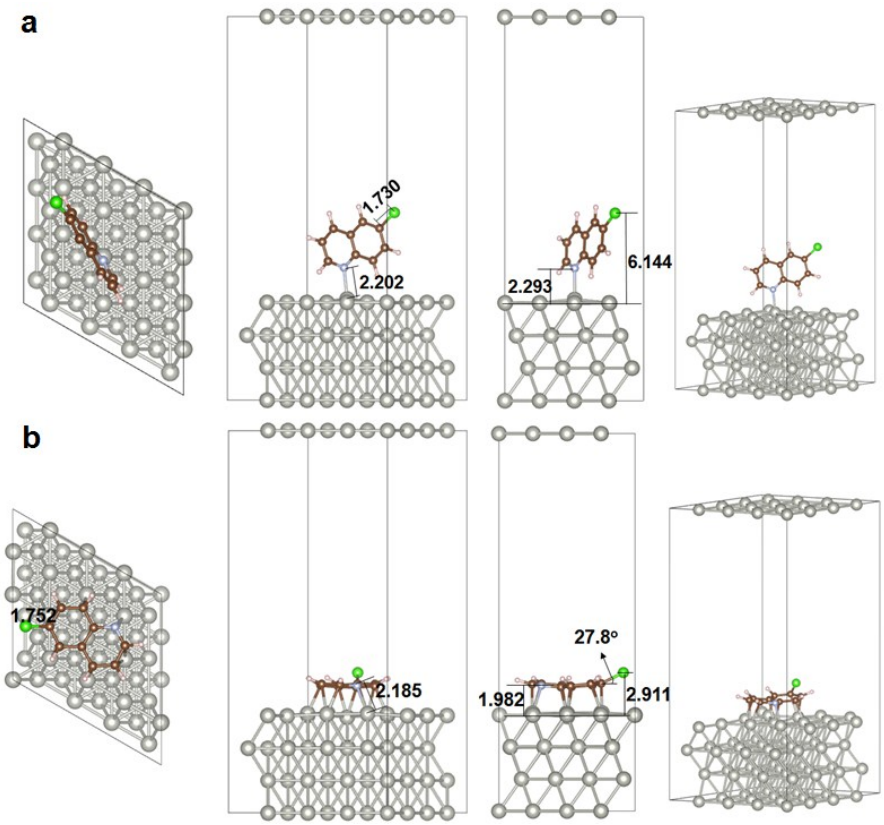

Figure S1. Summary of the adsorption configuration of 6-chloroquinoline molecule on Pd (111) crystal face: (a) Tilted configuration; (b) Flat configuration.

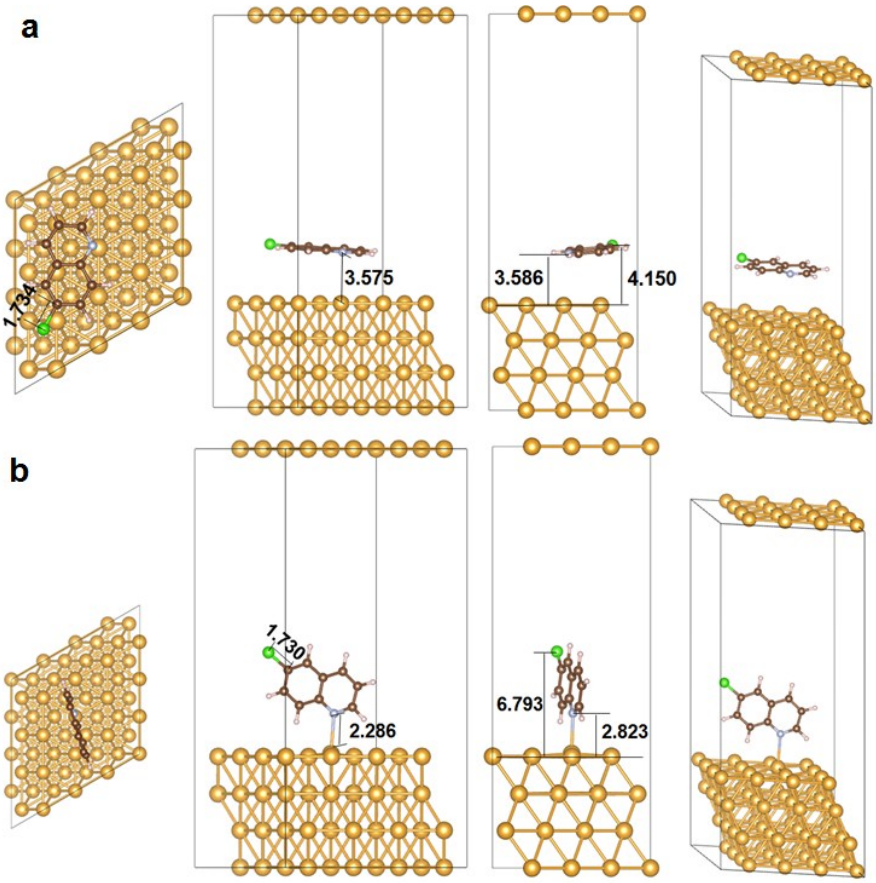

Figure S2. Summary of the adsorption configuration of 6-chloroquinoline molecule on Pd (111)crystal face: (a) Flat configuration; (b) Tilted configuration.

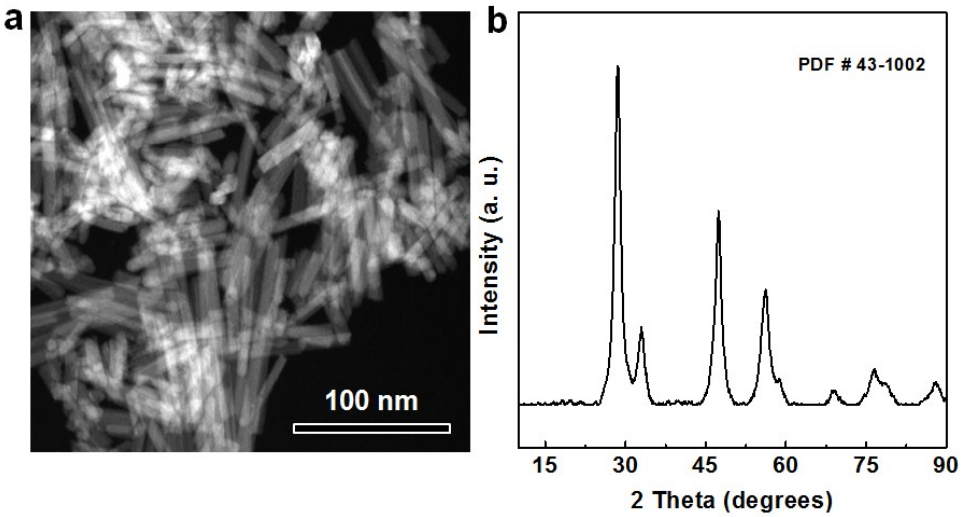

Figure S3. Structure characterizations of nanorods CeO_2. (a) Dark field TEM image and (b) XRD spectrum of nanorods CeO_2.

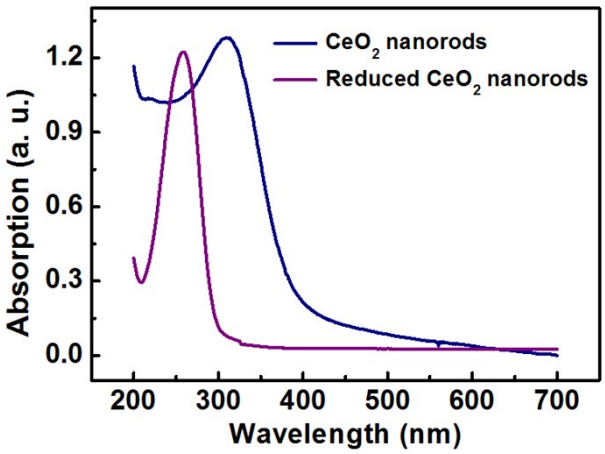

Figure S4. UV-vis absorption spectra of as-synthesized CeO_2 nanorods and the reduced CeO_2 nanorods by ascorbic acid.

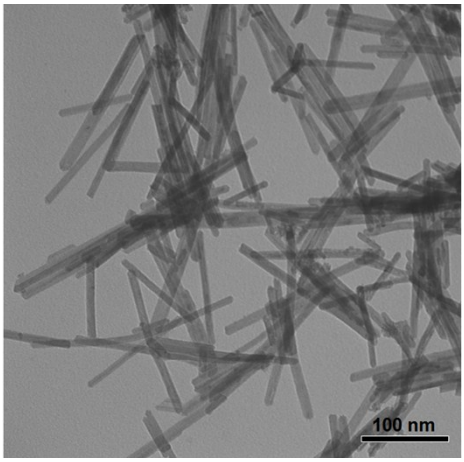

Figure S5. TEM image of CeO_2 nanorods after the chemical reduction by ascorbic acid.

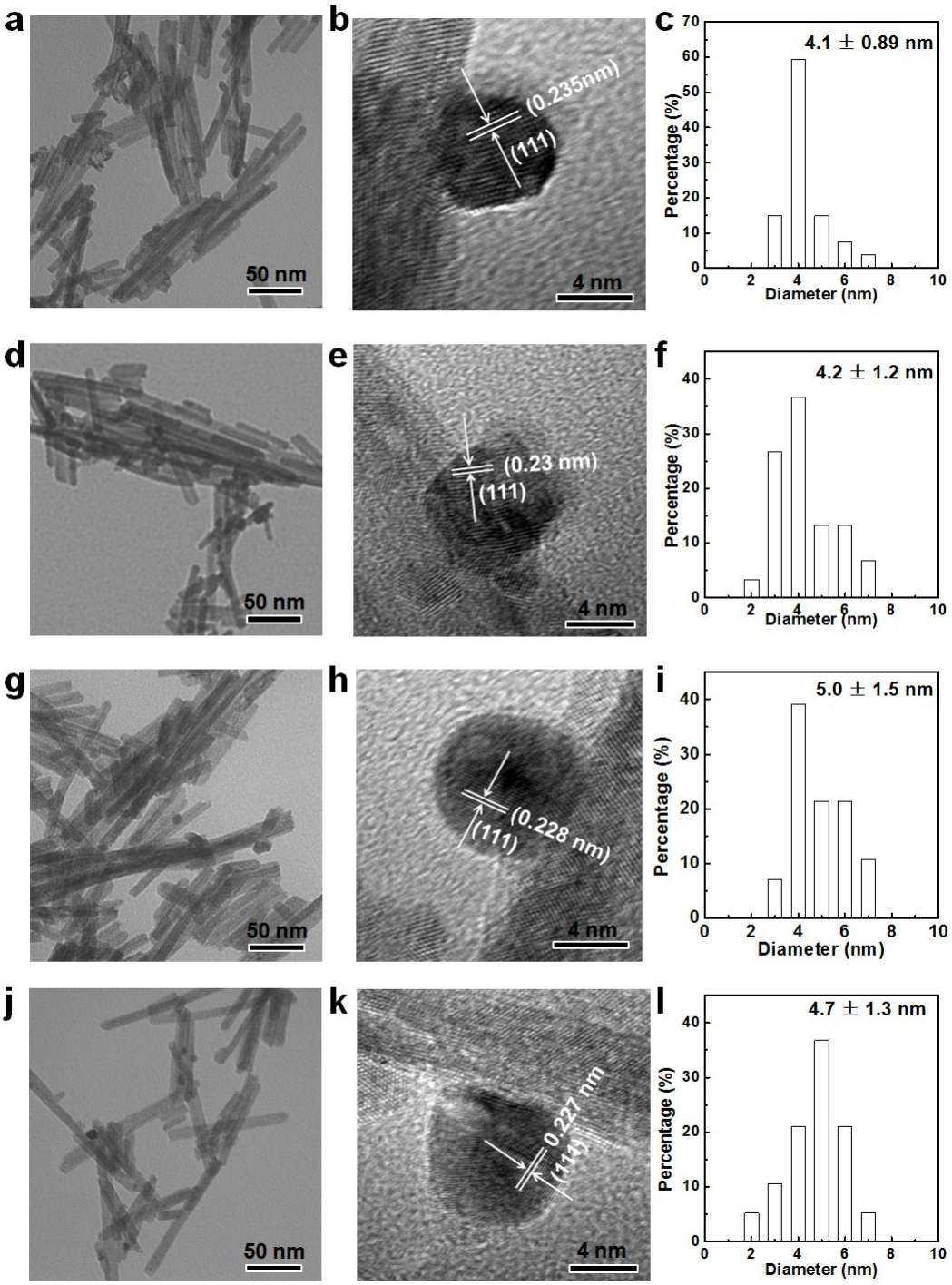

Figure S6. TEM images of (a) $Au_{0.93}Pd_{0.07}$/CNR, (b) $Au_{0.75}Pd_{0.25}$/CNR, (c) $Au_{0.4}Pd_{0.6}$/CNR, (d) $Au_{0.25}Pd_{0.75}$/CNR catalysts. Size distributions of all catalyst are shown in inset.

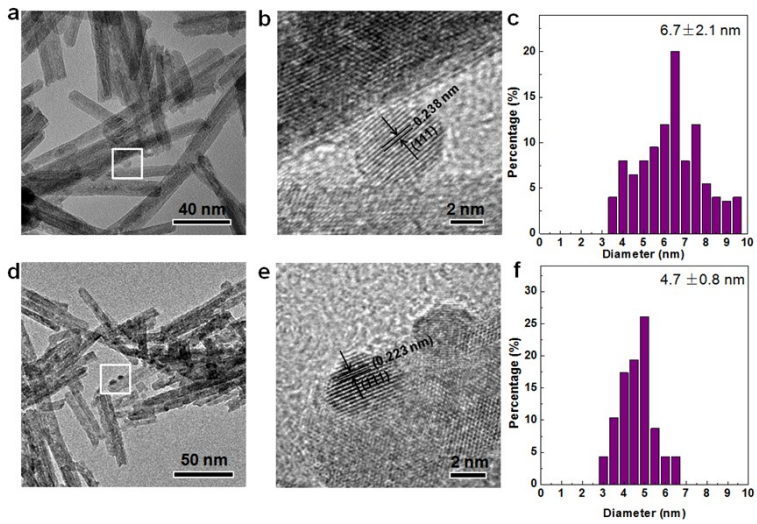

Figure S7. The Au/CNR catalyst: (a) TEM image, (b) HR-TEM image and (c) Size distribution of Au particles. The Pd/CNR catalyst: (d) TEM image, (e) HR-TEM image and (f) Size distribution of Pd particles.

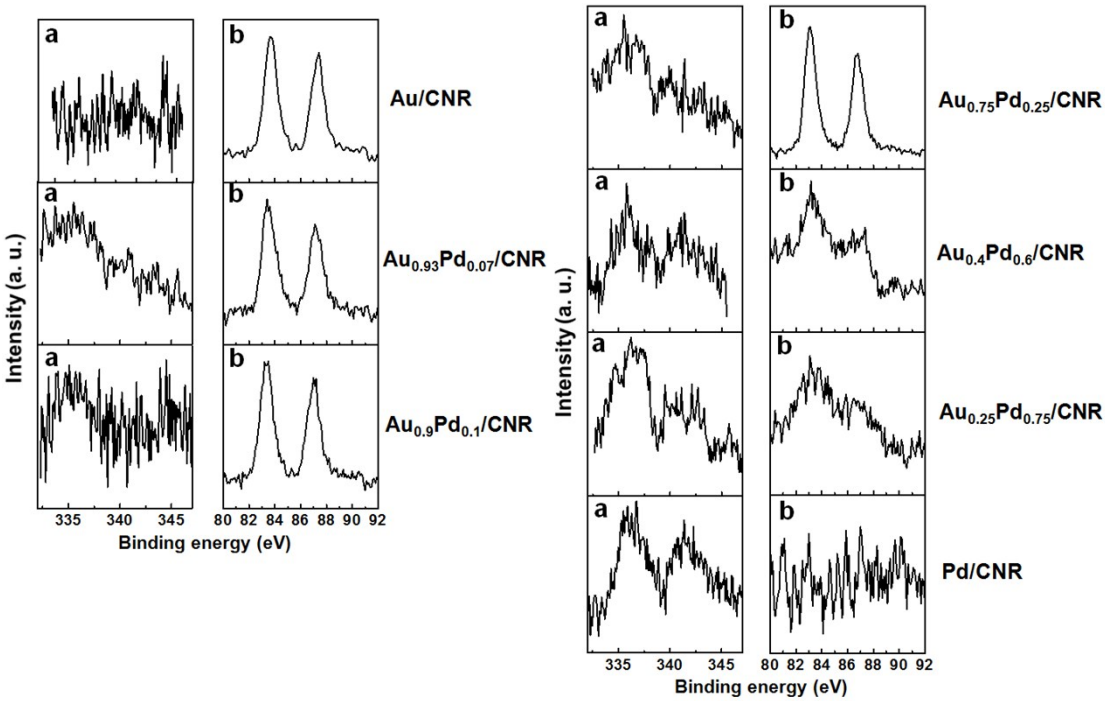

Figure S8. XPS spectrum of (a) Pd and (b) Au for various Au_xPd_{1-x}/CNR catalysts.

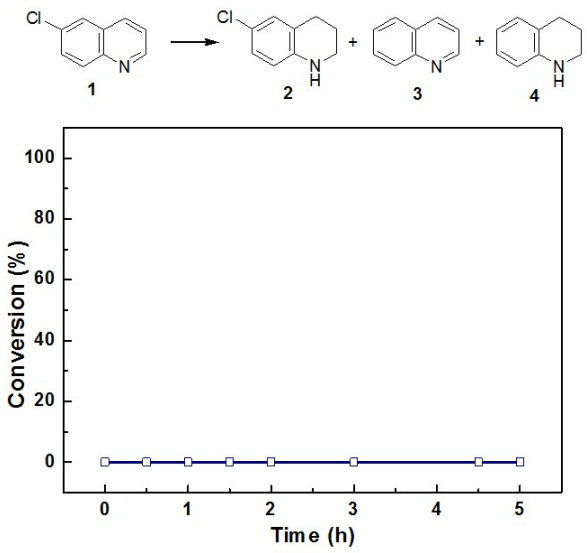

Figure S9. Time course of conversion of 6-chloroquinoline catalyzed by the Au/CNR catalyst. **Reaction conditions**: 6-chloroquinoline (0.2 mmol), Au/CNR catalysts (5 mg), toluene (2 mL), 100 °C and hydrogen pressure (2 MPa). Obviously, the Au/CNR catalysts exhibited no catalytic activity for hydrogenation of 6-chloroquinoline.

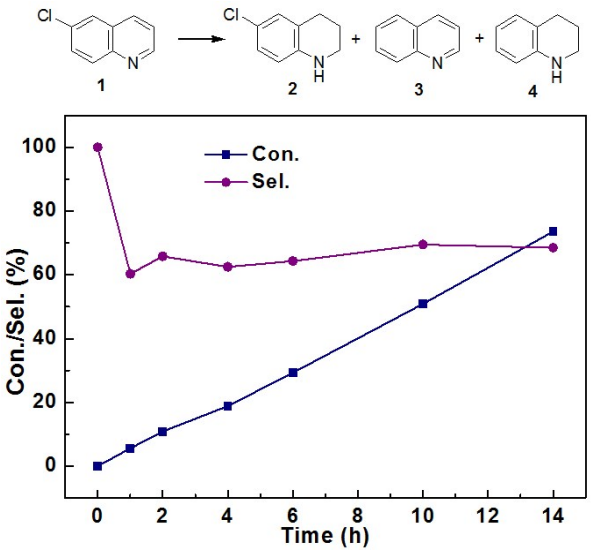

Figure S10. Catalytic performance of the Lindlar catalyst: Time course of conversion of 6-chloroquinoline (**1**) and selectivity of 6-chloro-1,2,3,4-tetrahydroquinoline (**2**). **Reaction conditions:** 0.2 mmol of 6-chloroquinoline, 10 mg of catalyst, 2 mL of toluene, 100 °C and 2 MPa H_2 pressure.

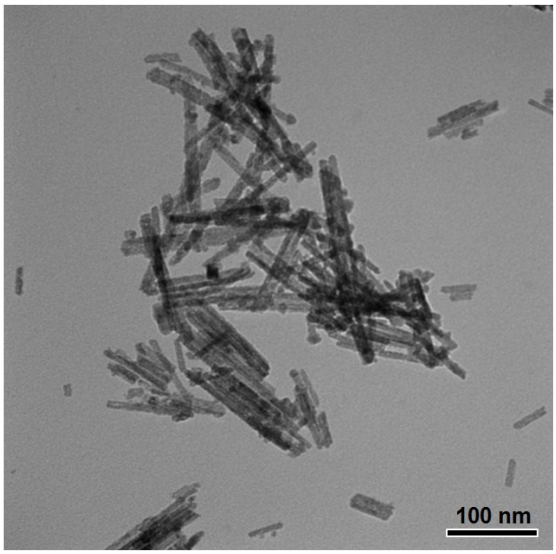

Figure S11. TEM image of the spent $Au_{0.9}Pd_{0.1}$/CNR catalysts.

Table S1. Summary of the selectivity or yield for the hydrogenation of functionalized quinolines in previously reported.

Entry	Catalyst	Substrates	Products	Selectivity/yield (%)
1	Rh nanopatrticles	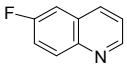	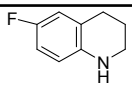	73 [1]
2	Au/TiO_2	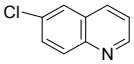	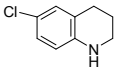	100 [2]
3	*N*-graphene modified cobalt nanoparticles	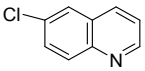	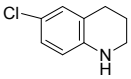	81 [3]
4	Co nanoparticles			0 [4]

Table S2. Optimization of the reaction conditions for hydrogenation of 6-chloroquinoline.

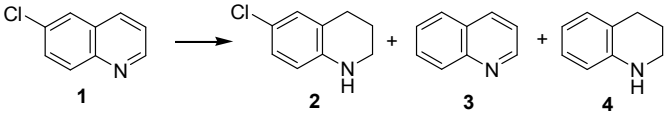

Entry	Temperature (°C)	Pressure (MPa)	Solvent	Time (h)	Con. (%)	Sel. (%)		
						2	3	4
1	90	2	H_2O	3	60.5	80.1	46.9	23.2
2	90	2	CH_3CN	3	19.5	53.4	41.5	5
3	90	2	THF	3	20.9	86.1	11.1	2.8
4	90	2	n-hexane	3	66.9	78.9	12.3	7.9
5	90	2	Toluene	3	74.3	82.6	13.6	3.8
6	100	2	Toluene	3	81.0	89.6	5.6	7.8
7	100	3	Toluene	3	93.8	84.0	9.1	6.9
8	100	1	Toluene	3	65.6	89.9	6.2	6.9

Reaction conditions: $Au_{0.9}Pd_{0.1}$/CNR (5 mg), 6-chloroquinoline (0.2 mmol) and solvent (2 mL).

References

(1) Karakulina, A.; Gopakumar, A.; Akcok, I.; Roulier, B. L.; LaGrange, T.; Katsyuba, S. A.; Das, S.; Dyson, P. J. *Angew. Chem. Int. Ed.* **2016**, *55*, 292.

(2) Ren, D.; He, L.; Yu, L.; Ding, R. S.; Liu, Y. M.; Cao, Y.; He, H. Y.; Fan, K. N. *J. Am. Chem. Soc.* **2012**, *134*, 17592.

(3) Chen, F.; Surkus, A. E.; He, L.; Pohl, M. M.; Radnik, J.; Topf, C.; Junge, K.; Beller, M. *J. Am. Chem. Soc.* **2015**, *137*, 11718.

(4) Nador, F.; Moglie, Y.; Vitale, C.; Yus, M.; Alonso, F.; Radivoy, G. *Tetrahedron* **2010**, *66*, 4318.